

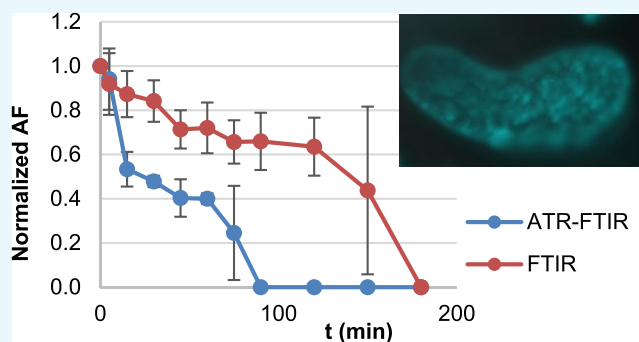
Kinetic Analysis of Cellulose Acetate/Cellulose II Hybrid Fiber Formation by Alkaline Hydrolysis

Najua Tulos,^{†,‡} David Harbottle,^{‡,§} Andrew Hebden,[§] Parikshit Goswami,[§] and Richard S. Blackburn^{*,†,§}

[†]Sustainable Materials Research Group, School of Design and [‡]School of Chemical and Process Engineering, University of Leeds, Leeds LS2 9JT, U.K.

[§]School of Applied Sciences, University of Huddersfield, Huddersfield HD1 3DH, U.K.

ABSTRACT: Cellulose acetate (CA) can be converted to cellulose II through a deacetylation process using ethanolic NaOH solution. Infrared spectroscopy was used to observe the degree of acetylation by comparing the absorption intensities of C=O and C–O stretches. Attenuated total reflection-Fourier transform infrared (ATR-FTIR) analysis, which only measures a few microns into the fiber diameter, was compared with FTIR, which measures the whole fiber cross-section. Steady deacetylation of the whole fiber over 180 min was observed with FTIR to eventual complete deacetylation. In comparison, ATR-FTIR shows deacetylation occurring more rapidly to complete deacetylation after 90 min, indicating rapid deacetylation of the CA fiber periphery. Data were fitted to a pseudo-second order kinetic model, with high correlation ($R^2 > 0.99$), and it was observed that the deacetylation rate (k_2) observed with ATR-FTIR (-0.634 min^{-1}) was twice as rapid as the deacetylation rate observed with FTIR (-0.315 min^{-1}). IR observations were in agreement with the analysis of fiber cross-sections by confocal microscopy, where it was observed that changes in fiber morphology occurred with treatment time and progressive hydrolysis of cellulose acetate to cellulose II. A differential fiber chemical composition was created within the CA fiber cross-section; after 5 min, the outer regions of the fiber cross-section are hydrolyzed to cellulose II and this hydrolysis increases heterogeneously with time to complete hydrolysis after 180 min and conversion to cellulose II. These results indicate the potential to produce fibers with a differential periphery/core structure, which can be accurately designed according to the relative degrees of cellulose II/CA required for specific applications by varying the treatment time in application of this model.



INTRODUCTION

Cellulose is a linear polymer composed of glucose units that are linked by β -1,4-glycosidic bonds formed between the carbon atoms C(1) and C(4) of adjacent glucose units. Cotton fibers are one of the purest sources of cellulose and the most important industrial natural fibers.¹ The demand for cellulose and its derivatives within the technical textile industry is high due to its outstanding properties, such as excellent moisture absorption, good abrasion resistance, and high strength. However, native cellulose (cellulose I β) has poor solubility in most solvents as a result of extensive hydrogen bonding between molecular chains, which forms a supramolecular structure that can be described by a two-phase model with regions of high orientation (crystalline) and low orientation (amorphous).^{2–6} This greatly restricts the development and utilization of cellulose and hence cellulose derivatives have been developed for use in fiber applications.

Cellulose acetate (CA) is one of the essential esters of cellulose obtained via an acetylation process, wherein cellulose is reacted with acetic anhydride and acetic acid in the presence of sulfuric acid.⁷ The properties of CA fibers mostly depend on solution viscosity and degree of esterification;^{8,9} the most

common form of CA fibers have a degree of substitution of 2.0–2.5 (secondary cellulose acetate)⁷ and these fibers are used in apparel because they are hygroscopic as the amorphous open-pore structure allows moisture to be transported away from the body, making the wearer feel cool and comfortable.^{10,11} When the degree of substitution reaches a low value of about 1.5, it leads to cellulose-like properties, wherein the polymer becomes more hydrophilic, accompanied by enhanced wettability and water sorption.^{6,9}

Deacetylation of CA fibers leads to the formation of cellulose II and can be commonly achieved with aqueous or alcoholic alkali solutions, which remove acetyl groups ($-\text{COCH}_3$). The degree of deacetylation and the time to achieve deacetylation depend on several factors, including solvent type, alkali concentration, and liquor to fiber ratio.^{12–14} Liu and Hsieh¹² demonstrated that deacetylation of cellulose acetate fibers with 0.05 M NaOH in ethanol was more efficient, homogenous, and

Received: January 17, 2019

Accepted: February 20, 2019

Published: March 6, 2019

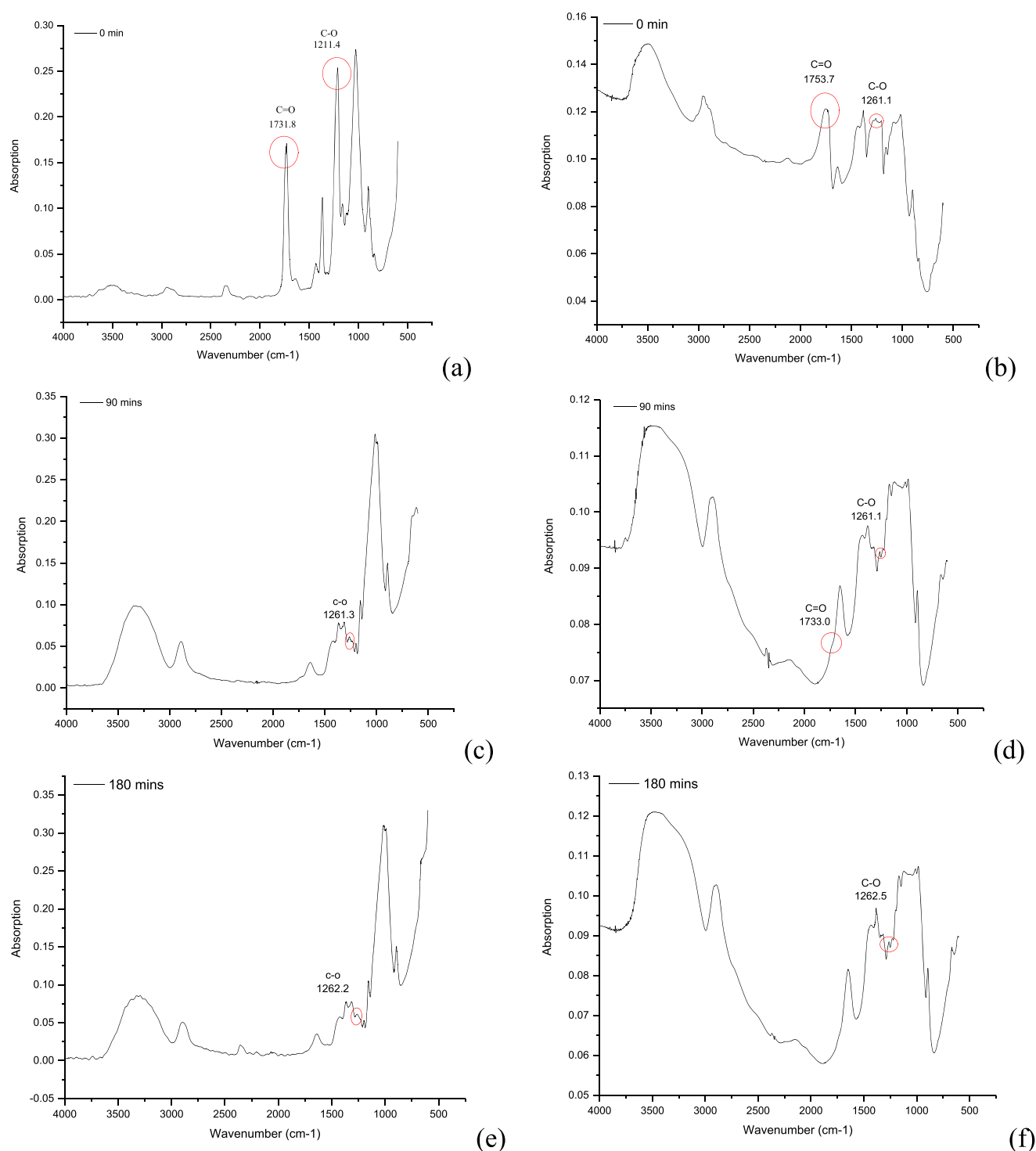


Figure 1. (a) ATR-FTIR spectrum for the CA fiber before deacetylation; (b) FTIR spectrum for the CA fiber before deacetylation; (c) ATR-FTIR spectrum for CA fiber after 90 min treatment; (d) FTIR spectrum for the CA fiber after 90 min treatment; (e) ATR-FTIR spectrum for the CA fiber after 180 min treatment; (f) FTIR spectrum for the CA fiber after 180 min treatment. Red circles indicate the C=O and C-O absorption bands.

complete than the same alkali concentration in aqueous conditions and found that conversion of ester into hydroxyl with progressive hydrolysis leads to improved wettability.

Cellulose is highly hygroscopic due to a high number of hydroxyl groups in its molecular structure; CA is more hydrophobic than cellulose, due to acetylation of the majority of hydroxyl functions, and hence water sorption is significantly reduced. As cellulose II and CA fibers have different moisture

sorption properties, the aim of this research is to produce differentiated cellulose II/cellulose acetate hybrid fibers, where the periphery of the fiber is composed of cellulose II and the core is CA. The intended application is that the resultant fibers will have smart thermoresponsive functions.

Infrared spectroscopy is used herein as the primary technique to monitor changes in the fibers. IR spectroscopy has been applied extensively over the past sixty years to study cellulose I

and cellulose II, and Fourier transform infrared (FTIR) spectroscopy has demonstrated a clear relationship between the interaction of hydroxyl groups and crystallinity. Using classic potassium bromide pellet FTIR techniques, O'Connor et al.¹⁵ first developed the “crystallinity index” for cellulose I, where absorption at 1429 cm^{-1} decreased and absorption at 893 cm^{-1} ($\alpha_{1429/893}$) increased as crystallinity decreased. Subsequently, the “lateral order index” (LOI; $\alpha_{1418/894}$),¹⁶ “total crystallinity index” (TCI; $\alpha_{1372/2900}$),¹⁷ and “hydrogen-bond intensity” (HBI; $\alpha_{3336/1336}$)¹⁸ have all been developed to study crystallinity in cellulose I and II, and partially mercerized cellulose. The Carrillo–Colom index ($\alpha_{1278/1263}$) was specifically developed to explain crystallinity changes in cellulose II polymers upon sodium hydroxide treatment.^{19,20}

More recently, researchers have used attenuated total reflectance-Fourier transform infrared (ATR-FTIR) spectroscopy to analyze crystallinity changes in cellulose I and cellulose II fibers and demonstrated a good comparison with analytical techniques such as X-ray diffraction (XRD). Kljun et al.²¹ found that ATR-FTIR offered a reliable and useful way of monitoring and quantifying crystallinity and morphological changes in developing cotton (cellulose I) fibers and used LOI to show that significant increases in crystallinity occur between days 17 and 26 post-anthesis; HBI was used to observe significant changes in intermolecular hydrogen bonds from anthesis to day 60. Kljun et al.²² also found that ATR-FTIR compared well with XRD in quantifying crystallinity changes in cellulose I and its conversion to cellulose II upon treatment with various concentrations of sodium hydroxide. Široký et al.^{23,24} demonstrated that ATR-FTIR spectroscopy could be used to monitor crystallinity and morphological changes in cellulose II polymer fibers when treated with varying concentrations of alkali; they demonstrated that TCI, LOI, and HBI could all be used to understand which alkali concentrations were responsible for reorganization in the amorphous and quasicrystalline phases of cellulose II fibers. The researchers also demonstrated the advantages in using in situ fiber measurement with ATR-FTIR.

RESULTS AND DISCUSSION

Cellulose acetate can be converted to cellulose II through an alkaline deacetylation process. Infrared (IR) spectroscopy techniques were used to analyze changes in the chemical composition of CA fibers as a function of NaOH treatment time, specifically the removal of CA acetyl groups. The diameter of the as-spun CA fibers ranged from 21.6 to $34.7\text{ }\mu\text{m}$. ATR-FTIR can only measure up to a few microns (0.5 – $5.0\text{ }\mu\text{m}$) into the fiber diameter²³ and hence the measurement is more sensitive to changes at the surface rather than in the bulk. Differences in the analytical techniques, FTIR and ATR-FTIR, could be used to compare the chemical characteristics of the periphery of the fiber (ATR-FTIR) and the whole fiber cross-section (FTIR). CA fibers show characteristic IR absorption bands at around 1760 – 1730 cm^{-1} , corresponding to the overlapped ester carbonyls, and this $\text{C}=\text{O}$ band may be used to observe the degree of acetylation. The $\text{C}-\text{O}-\text{C}$ band at 1162 – 1125 cm^{-1} was used for normalization as it is unchanged in intensity during deacetylation. Relative absorption intensities of the $\text{C}=\text{O}$ stretch at 1760 – 1730 cm^{-1} and the $\text{C}-\text{O}$ stretch at 1270 – 1210 cm^{-1} , both corresponding to the acetyl group, were used to determine the relative degrees of CA and cellulose II content and to compare the analyses by ATR-FTIR and FTIR.¹²

Figure 1 shows the changes in the ATR-FTIR and FTIR spectra before and during deacetylation. It can be seen that there

is a difference in absorption intensities in FTIR and ATR-FTIR spectra for the $\text{C}=\text{O}$ and $\text{C}-\text{O}$ peaks; this is attributed to the difference in penetration of IR light into the sample. FTIR is also able to measure spectra with high signal-to-noise ratios which leads to a high-intensity infrared spectrum.²⁵ An intense carbonyl peak is observed in both FTIR and ATR-FTIR spectra before deacetylation but with alkali treatment, the $\text{C}=\text{O}$ band slowly diminishes. After 90 min, the carbonyl is still identified in the core of the fiber, which suggests a difference in the acetyl content between the periphery and the core of the fiber; cellulose II is formed at the surface, whereas CA is still present at the core. After 180 min, the $\text{C}=\text{O}$ band is completely absent, indicative of full deacetylation. The relationship between FTIR and ATR-FTIR spectra, i.e., the difference in the chemistry of the peripheral layer of the fiber compared to the chemistry of the whole fiber cross-section, is articulated in this study by the acetyl factor (AF); to the best of our knowledge, this is the first time that the acetyl factor has been used to articulate such a difference.

Herein, we have defined the term acetyl factor (AF) as the ratio of sorption intensity for the $\text{C}=\text{O}$ group to the sorption intensity of the $\text{C}-\text{O}$ group (eq 1).

$$\text{AF} = \frac{\text{absorption intensity of C}=\text{O}}{\text{absorption intensity of C}-\text{O}} \quad (1)$$

We propose that this equation may be used to indicate the degree of acetylation of the treated fibers since $\text{C}=\text{O}$ groups are affected by deacetylation and the $\text{C}-\text{O}$ groups are not. The normalized acetyl factor ($\overline{\text{AF}}$) is given by eq 2

$$\overline{\text{AF}} = \frac{\text{AF}}{\text{AF}_0} \quad (2)$$

where AF_0 is the initial acetyl factor.

Figure 2 shows $\overline{\text{AF}}$ for both ATR-FTIR and FTIR measurements as a factor of treatment time (t). It is observed

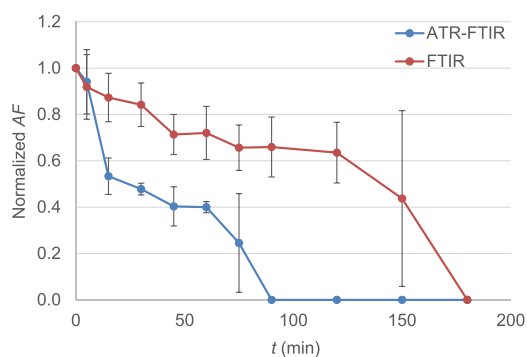


Figure 2. Normalized acetyl factor for the CA fiber as a factor of treatment time.

with FTIR that $\overline{\text{AF}}$ decreases steadily over 180 min, indicating steady deacetylation of the whole fiber to eventual complete deacetylation. For ATR-FTIR, $\overline{\text{AF}}$ decreases more rapidly than the $\overline{\text{AF}}$ measured by FTIR, with $\overline{\text{AF}} = 0$ at $t = 90$ min, indicating rapid deacetylation of the CA fiber periphery (up to $5\text{ }\mu\text{m}$ from the fiber surface) in half the time to achieve complete deacetylation of the whole fiber.

The data in Figure 2 were fitted to a pseudo-second order kinetic model, as described by eq 3

$$\frac{\partial AF_t}{\partial t} = k(AF_e - AF_t)^2 \quad (3)$$

where AF_t and AF_e are the acetyl factors of the fiber at a given time (t) and at equilibrium, respectively (no units). The term k_2 is the rate constant of the pseudo-second-order equation (min^{-1}). For boundary conditions $t = 0$ to $t = t$ and $AF_t = 0$ to $AF_t = AF_e$, the integrated form of eq 3 becomes eq 4

$$\frac{t}{AF_t} = \frac{1}{kAF_e^2} + \frac{1}{AF_e}t \quad (4)$$

Plotting t/AF_t against t produces a straight line, where the absorbance at equilibrium (AF_e) = 1/slope, and the pseudo-second-order rate constant (k_2) = slope²/intercept. Figure 3

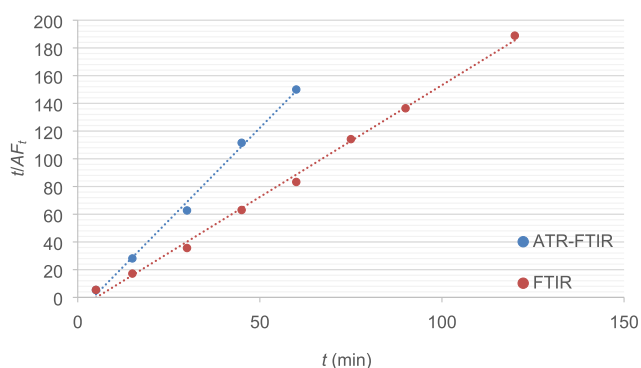


Figure 3. Pseudo-second-order model (t/AF_t vs t) for AF of the CA fiber as a factor of treatment time.

shows a high correlation ($R^2 > 0.99$) of the data with the pseudo-second-order model, where it is observed that for ATR-FTIR, $k_2 = -0.634 \text{ min}^{-1}$ and for FTIR, $k_2 = -0.315 \text{ min}^{-1}$, indicating that the rate of deacetylation at the surface of the fiber (as evidenced through ATR-FTIR investigation) is approximately twice the rate of deacetylation for the total fiber (as evidenced through FTIR investigation). These results indicate the potential to produce fibers with a differential periphery/core structure, which can be accurately designed according to the relative degrees of cellulose II/CA required for specific applications by varying the treatment time in application of this model.

Cross-sectional confocal microscopy of the cellulose II/CA fiber at different stages of the deacetylation process (Figure 4) shows changes in fiber morphology during progressive hydrolysis. The images suggest that there is a differential fiber chemical composition created within the CA fiber cross-section, as evidenced by staining with calcofluor fluorescent white (CFW). The stain does not bind with CA, so initially there is no staining of the fiber though the cross-section (a). After 5 min of treatment (b), staining at the fiber periphery is observed, which indicates that the outer regions of the fiber cross-section have been hydrolyzed to cellulose II, in agreement with the findings from IR analysis (Figure 2). Staining with CFW increases heterogeneously with time, suggesting that a pore structure through the fiber cross-section allows the ethanolic NaOH solution to enter the amorphous regions, enabling deacetylation to take place. Prolonged immersion in the ethanolic NaOH solution allows complete hydrolysis, where it is observed after 180 min (e) that the whole fiber cross-section is stained with CFW, indicating complete conversion to cellulose II; again, this is in agreement with IR analysis findings.

The kinetics discussed herein consider the rate of deacetylation at the periphery of the fiber compared to the whole cross-section, and hence, this does not consider the differences in the cross-sectional shape. As ATR-FTIR can only measure up to $5 \mu\text{m}$ from one side of the fiber, and the narrowest diameter of any fiber observed herein was $12 \mu\text{m}$, the conclusions comparing diffusion at the periphery of the fiber and the whole fiber remain valid, even though the fibers are not a perfect circular cross-section. If the fibers were perfectly circular, this may affect absolute kinetics as the narrowest part of the fiber cross-section may be different (wider) but this would not change the fundamental principles observed.

MATERIALS AND METHODS

Materials. Cellulose acetate ($M_w = 30\,000$, 39.8% acetyl content), acetone ($\geq 99\%$), sodium hydroxide (NaOH; $\geq 97\%$), hydrochloric acid (HCl; $\geq 37\%$), and calcofluor fluorescent white (CFW) were purchased from Sigma-Aldrich, U.K. Ethanol absolute (EtOH; $\geq 99.8\%$) was procured from VMR Chemicals, U.K. All other general purpose chemicals were purchased from Sigma-Aldrich, U.K.

Wet Spinning of Cellulose Acetate. Wet spinning was used to produce CA fibers. This process is based on precipitation, where a polymer is extruded through a spinneret into a liquid coagulating bath to yield solid filaments.²⁶ The solidified fiber undergoes washing, chemical treatment, drawing, and a drying process before being wound up onto a bobbin.^{27,28} Extrusion into liquid exerts a drag force on the filament; once the solvents are evaporated, the filaments are drawn or stretched to orient the molecular chains to give the fiber its strength.²⁶ Figure 5 shows a schematic representation of the wet spinning line used in this research, which consists of three main units: (unit A) spinning unit with dope supply reservoir and coagulation bath; (unit B) washing, drawing, and drying unit; and (unit C) receiving bobbin for collecting the fiber produced. The spinning dope was prepared by dissolving CA (17.0 g) in acetone (100 mL) with constant stirring at room temperature ($25 \pm 5 \text{ }^\circ\text{C}$) for 24 h. The spinning solution was extruded through a 0.1 mm diameter spinneret (100 holes), with a pump speed of 40 rpm, into a coagulation bath containing distilled water at $25 \text{ }^\circ\text{C}$ (unit A). Subsequently, the fibers were washed in a bath containing distilled water at $25 \text{ }^\circ\text{C}$ (unit B, zone 1), whilst simultaneously being drawn at a differential speed ratio of 1:1.10; then washed in a bath containing distilled water at $25 \text{ }^\circ\text{C}$ (unit B, zone 2), whilst simultaneously being drawn at a differential speed ratio of 1:1.09; then dried in air at $40 \text{ }^\circ\text{C}$ (unit B, zone 3), whilst simultaneously being drawn at a differential speed ratio of 1:1.08. Finally, the fibers were taken up on the winder roller at a winding speed of $90\text{--}110 \text{ m min}^{-1}$ (unit C).

Deacetylation of Cellulose Acetate Wet-Spun Fibers. Deacetylation was carried out to remove acetyl groups from the as-spun CA fibers by alkaline hydrolysis at room temperature using a Mathis Airboy Dyeing Machine. CA fibers were wound over a metal frame and loaded into glass dyeing tubes containing 1.0 M ethanolic NaOH solution (100 mL). Fiber samples were treated at $21 \text{ }^\circ\text{C}$ for treatment times ranging from 0 to 180 min. After treatment, the fibers were rinsed and treated in 0.1 N aqueous HCl solution (100 mL) for 10 min, followed by rinsing with tap water. The fibers were then dried in air at room temperature for 3 h.

Fiber Cross-Section Area Measurements. The fiber cross-section was imaged by using a light microscope, Leica M205C, equipped with a TL BFDF transmitted-light stand and a

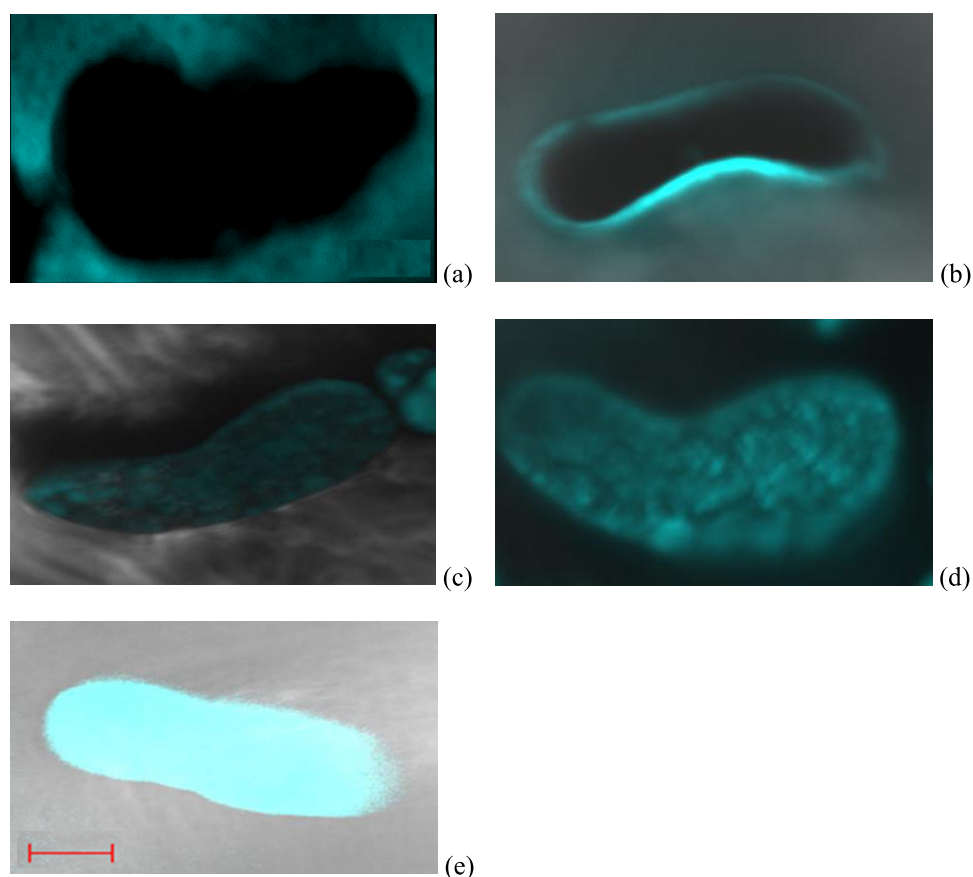


Figure 4. Cross-sectional confocal microscopy of the cellulose II/CA fiber after treatment with ethanolic NaOH solution for (a) 0 min, (b) 5 min, (c) 30 min, (d) 90 min, and (e) 180 min. The scale bar is 10 μm .

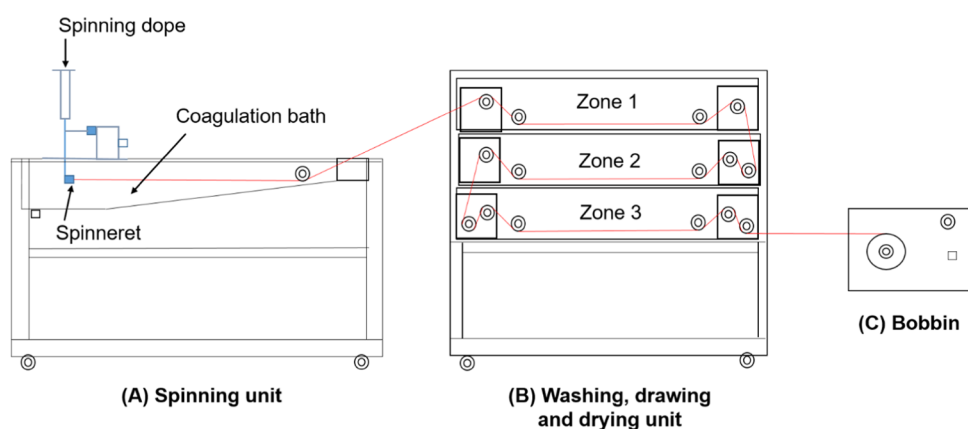


Figure 5. Schematic diagram of a wet spinning machine: unit A is the spinning unit; unit B is for washing and drawing (zones 1 and 2) and drying and drawing (zone 3); unit C is the receiving bobbin.

manual focusing drive. Image analysis software, Image J, was used to view and measure the fiber cross-section area before and after deacetylation.

Fourier Transform Infrared (FTIR) Spectroscopy. Prior to analysis, the fibers were conditioned at $65 \pm 2\%$ relative humidity and $20 \pm 2^\circ\text{C}$ for 48 h. Spectroscopic grade potassium bromide (KBr) powder was dried in an oven at 100°C for 1 h. Fiber samples were mixed with dried potassium bromide powder in a 1:9 ratio, placed into a mortar and ground with an agate pestle until the sample was well dispersed and the mixture has the consistency of a fine powder. The ground powder was placed in a die assembly and transferred to a hydraulic press. Air was

removed from the sample under high vacuum for 2 min and then pressed at 281 kg cm^{-2} for 1 min, after which the pressure was released. The pressed sample was removed from the die and placed into the FTIR sample holder. The samples were subjected to FTIR spectroscopy using a PerkinElmer Spectrum BX spotlight spectrophotometer. Scanning was conducted from 4000 to 600 cm^{-1} with 64 scans averaged for each spectrum. The resolution was 4 cm^{-1} and interval scanning was 2 cm^{-1} .

Attenuated Total Reflectance-Fourier Transform Infrared (ATR-FTIR) Spectroscopy. A detailed description of the use of ATR-FTIR spectroscopy for analyzing cellulosic fibers is given by Široký et al.²³ Prior to analysis, the fibers were

conditioned at 65 ± 2% relative humidity and 20 ± 2 °C for 48 h. The samples were subjected to FTIR spectroscopy (at four different points in the sample) using a PerkinElmer Spectrum BX spotlight spectrophotometer with a diamond ATR attachment. Scanning was conducted from 4000 to 600 cm⁻¹ with 64 scans averaged for each spectrum. The resolution was 4 cm⁻¹ and interval scanning was 2 cm⁻¹. The angle of incidence of the IR beam was 45° and the depth of penetration was approximately 0.5–5.0 μm.

Confocal Microscopy. The samples were washed in phosphate-buffered saline at least three times and incubated with cellulose stain CFW (0.2 g mL⁻¹) for 5 min in the dark. Objective EC Plan-Neofluar Oil was added to the samples to provide clearer imaging. Labeled samples were visualized with an epifluorescence microscope (Eclipse E600, Nikon, U.K.). Images were observed by a Zeiss LSM880 Confocal Microscope equipped with Airyscan under 20× and 40× magnification. Images were captured and analyzed with a ZEN Digital Imaging for Light Microscopy Black Edition. The images were then exported in TIFF format and the final images were edited using the ZEN Black software. CFW binds strongly to 1,3- and 1,4-polysaccharides but does not bind to CA and was used herein to identify differential regions of the fibers between cellulose II and CA.²⁹

AUTHOR INFORMATION

Corresponding Author

*E-mail: r.s.blackburn@leeds.ac.uk. Phone: +44 113 343 3757.

ORCID

David Harbottle: 0000-0002-0169-517X

Richard S. Blackburn: 0000-0001-6259-3807

Present Address

¹Faculty of Applied Sciences, Universiti Teknologi MARA, 40450 Shah Alam, Selangor, Malaysia

Author Contributions

The manuscript was written through contributions of all authors. All authors have given approval to the final version of the manuscript.

Notes

The authors declare no competing financial interest.

ACKNOWLEDGMENTS

The authors would like to acknowledge the financial support from the Ministry of Education of Malaysia and Universiti Teknologi MARA (UiTM) for the provision of a Ph.D. scholarship to N.T.

REFERENCES

- (1) Hsieh, Y. L. *Cotton: Science and Technology*; Gordon, S., Hsieh, Y. L., Eds.; Woodhead: Cambridge, 2007.
- (2) Krässig, H. A. *Cellulose: Structure, Accessibility and Reactivity*; Krässig, H. A., Ed.; Gordon and Breach Science Publishers S. A.: Yverdon, 1993.
- (3) Frey, M. W. Electrospinning Cellulose and Cellulose Derivatives. *Polym. Rev.* **2008**, *48*, 378–391.
- (4) Kang, K. S.; Cho, K. Y.; Lim, H. K.; Kim, J. Investigation of Surface Morphology of Cellulose Acetate Micro-mould After Deacetylation. *J. Phys. D: Appl. Phys.* **2008**, *41*, No. 195403.
- (5) Li, X.; Li, N.; Xu, J.; Duan, X.; Sun, Y.; Zhao, Q. Cellulose Fibers from Cellulose/1-Ethyl-3-Methylimidazolium Acetate Solution by Wet Spinning with Increasing Spinning Speeds. *J. Appl. Polym. Sci.* **2014**, *131*, No. 40225.

(6) Isik, M.; Sardon, H.; Mecerreyes, D. Ionic Liquids and Cellulose: Dissolution, Chemical Modification and Preparation of New Cellulosic Materials. *Int. J. Mol. Sci.* **2014**, *15*, 11922–11940.

(7) Fischer, S.; Thümmel, K.; Volkert, B.; Hettrich, K.; Schmidt, I.; Fischer, K. Properties and Applications of Cellulose Acetate. *Macromol. Symp.* **2008**, *262*, 89–96.

(8) Goodlett, V. W.; Dougherty, J. T.; Patton, H. W. Characterizations of Cellulose Acetate by Nuclear Magnetic Resonance. *J. Polym. Sci., Part A-1: Polym. Chem.* **1971**, *9*, 155–161.

(9) Schaller, J.; Meister, F.; Schulze, T.; Krieg, M. Novel Absorbing Fibres Based on Cellulose Acetate. *Lenzinger Ber.* **2013**, *91*, 77–83.

(10) Law, R. C. Applications of Cellulose Acetate – Cellulose Acetate in Textile Application. *Macromol. Symp.* **2004**, *208*, 255–266.

(11) Pocienė, R.; Žemaitaitienė, R.; Vitkauskas, A. Mechanical Properties and Physical-chemical Analysis of Acetate Yarns. *Mater. Sci.-Medzg.* **2004**, *10*, 75–79.

(12) Liu, H.; Hsieh, Y.-L. Ultrafine Fibrous Cellulose Membranes from Electrospinning of Cellulose Acetate. *J. Polym. Sci., Part B: Polym. Phys.* **2002**, *40*, 2119–2129.

(13) Callegari, G.; Tyomkin, I.; Kornev, K. G.; Neimark, A. V.; Hsieh, Y.-L. Absorption and Transport Properties of Ultra-Fine Cellulose Webs. *J. Colloid Interface Sci.* **2011**, *353*, 290–293.

(14) He, X. Optimization of Deacetylation Process for Regenerated Cellulose Hollow Fiber Membranes. *Int. J. Polym. Sci.* **2017**, No. 3125413.

(15) O'Connor, R. T.; DuPré, E. F.; Mitcham, D. Applications of Infrared Absorption Spectroscopy to Investigations of Cotton and Modified Cottons: Part I: Physical and Crystalline Modifications and Oxidation. *Text. Res. J.* **1958**, *28*, 382–392.

(16) Hurtubise, F. G.; Krässig, H. Classification of Fine Structural Characteristics in Cellulose by Infrared Spectroscopy. Use of Potassium Bromide Pellet Technique. *Anal. Chem.* **1960**, *32*, 177–181.

(17) Nelson, M. L.; O'Connor, R. T. Relation of certain infrared bands to cellulose crystallinity and crystal lattice type. Part II. A new infrared ratio for estimation of crystallinity in celluloses I and II. *J. Appl. Polym. Sci.* **1964**, *8*, 1325–1341.

(18) Nada, A.-A. M. A.; Kamel, S.; El-Sakhawy, M. Thermal behaviour and infrared spectroscopy of cellulose carbamates. *Polym. Degrad. Stab.* **2000**, *70*, 347–355.

(19) Colom, X.; Carrillo, F. Crystallinity Changes in Lyocell and Viscose-Type Fibers by Caustic Treatment. *Eur. Polym. J.* **2002**, *38*, 2225–2230.

(20) Carrillo, F.; Colom, X.; Suñol, J. J.; Saurina, J. Structural FTIR Analysis and Thermal Characterisation of Lyocell and Viscose-Type Fibers. *Eur. Polym. J.* **2004**, *40*, 2229–2234.

(21) Kljun, A.; Benians, T. A. S.; Goubet, F.; Meulewaeter, F.; Knox, J. P.; Blackburn, R. S. Analysis of the Physical Properties of Developing Cotton Fibers. *Eur. Polym. J.* **2014**, *51*, 57–68.

(22) Kljun, A.; Benians, T. A. S.; Goubet, F.; Meulewaeter, F.; Knox, J. P.; Blackburn, R. S. Comparative Analysis of Crystallinity Changes in Cellulose I Polymers Using ATR-FTIR, X-ray Diffraction, and Carbohydrate-Binding Module Probes. *Biomacromolecules* **2011**, *12*, 4121–4126.

(23) Široký, J.; Blackburn, R. S.; Bechtold, T.; Taylor, J.; White, P. Attenuated total reflectance Fourier-transform Infrared spectroscopy analysis of crystallinity changes in lyocell following continuous treatment with sodium hydroxide. *Cellulose* **2010**, *17*, 103–115.

(24) Široký, J.; Benians, T. A. S.; Russell, S. J.; Bechtold, T.; Knox, J. P.; Blackburn, R. S. Analysis of Crystallinity Changes in Cellulose II Polymers Using Carbohydrate-Binding Modules. *Carbohydr. Polym.* **2012**, *89*, 213–221.

(25) Smith, B. C. *Fundamentals of Fourier Transform Infrared Spectroscopy*, 2nd ed.; CRC Press: Boca Raton, 2011.

(26) Lipscomb, A. G. *Cellulose Acetate, Its Manufacture and Applications*; E. Benn: London, 1933.

(27) Lewin, M.; Pearce, E. M. *Handbook of Fiber Chemistry*, 2nd ed.; Marcel Dekker: New York, 1998.

(28) Eichhorn, S. J.; Hearle, J. W. S.; Jaffe, M.; Kikutani, T. *Handbook of Textile Fibre Structure, Volume 1 - Fundamentals and Manufactured Polymer Fibres*, 1st ed.; Woodhead Publishing: Cambridge, 2009.

(29) Rasconi, S.; Jobard, M.; Jouve, L.; Sime-Ngando, T. Use of Calcofluor White for Detection, Identification, and Quantification of Phytoplanktonic Fungal Parasites. *Appl. Environ. Microbiol.* **2009**, *75*, 2545–2553.